https://doi.org/10.5194/egusphere-2025-3332
Preprint. Discussion started: 28 July 2025

Polyphase tectonic, thermal and burial history of the Vocontian basin revealed by U-Pb calcite dating

Louise Boschetti[1], Malou Pelletier[1], Frédéric Mouthereau[1,2], Stephane Schwartz[3], Yann Rolland[3,4], Guilhem Hoareau[5], Thierry Dumont[3], Dorian Bienveignant[3], Abdeltif Lahfid[6]

1. Géosciences Environnement Toulouse, Université de Toulouse Paul Sabatier, CNRS, IRD, 14 av. Edouard Belin, 31400 Toulouse, France
2. Institut Universitaire de France, F-75005 Paris, France
3. ISTerre, Université Grenoble Alpes, USMB, CNRS, IRD, UGE, 38000 Grenoble, France.
4. EDYTEM, Université Savoie Mont Blanc, CNRS, UMR 5204, Le Bourget du Lac, France.
5. Université de Pau et des Pays de l'Adour, E2S UPPA, CNRS, LFCR, UMR5150, Pau, France.
6. BRGM, B.P. 6009, 45060 Orléans Cedex, France

Corresponding author: louise.boschetti@univ-tlse3.fr

Abstract

The Vocontian Basin in southeastern France records a long-lived history of subsidence and polyphase deformation at the junction of Alpine and Pyrenean orogenic systems. This study aims to reconstructed the geodynamical evolution of this basin, based on new U–Pb dating of calcite from veins and faults combined with RSCM thermometry and stratigraphy-based burial models. Three main generations of calcites are dated: (1) Late Cretaceous to Paleocene dates related to Pyrenean-Provençal convergence (~84–50 Ma); (2) Oligocene dates linked to the West European Rift extension (~30–24 Ma); and (3) Miocene dates ascribed to strike-slip and compression associated with Alpine collision (~12–7 Ma). No older ages related to the Jurassic and Early Cretaceous rifting phases are obtained suggesting limited syn-rift fluid circulation or subsequent dissolution of early calcite mineralization. RSCM data highlight a pronounced E–W thermal gradient, with peak temperatures exceeding 250°C in the eastern basin, consistent with crustal thinning and/or salt diapirism. These results emphasize the large-scale impact of the opening of the West European Rift in SE France and underscore the possible mismatch

https://doi.org/10.5194/egusphere-2025-3332
Preprint. Discussion started: 28 July 2025

between the large-scale tectonics and the tectonic history inferred from calcite U–Pb dating, which is sensible to presence of fluids and the physical conditions for their preservations.

1. Introduction

Sedimentary basins located in the external part of orogenic belts can provide critical insights into the polyphase and complex evolution of tectonic plate boundaries. The Vocontian Basin in southeastern France is currently positioned at the front of the southern Alpine belt, to the north of Provence (Fig. 1). This basin recorded a succession of tectonic events spanning from the Late Cretaceous to the Cenozoic (Roure et al., 1992; Homberg et al., 2013; Mouthereau et al., 2021) (Fig. 1). These different tectonic events have been attributed to the Mesozoic rifting associated with the opening of the Alpine Tethys and the Atlantic Ocean-Pyrenean rift, Cenozoic inversion of the rifted margins during the development of the Pyrenees-Provence collision and the Eocene-Oligocene to Miocene extension associated with the opening of the West European Rift and the Gulf of Lion (e.g., Stämpfli, 1993; Homberg et al., 2013; Bestani et al., 2016; Espurt et al., 2019; Célini et al., 2023). Some details of the tectonic evolution of the Vocontian basin, positioned at the intersection between the Europe-Iberia and Europe-Adria plate boundaries are however debated. A long-standing debate persists on whether the Mid-Cretaceous Vocontian Basin, north of Provence, is part of a continuous rift system between the Valaisan/Alpine Tethys in the east and the Pyrenean/Atlantic Ocean in the west (Trümpy, 1988; Stämpfli, 1993; Stämpfli and Borel, 2002; Turco et al., 2012). In contrast, other studies suggest that the Vocontian Basin, while belonging to the broader Pyrenean/Atlantic rift system, remained structurally disconnected from other Pyrenean and Provençal rift segments (Debelmas, 2001; Manatschal and Muntener, 2009; Angrand and Mouthereau, 2021; Célini et al., 2023; Boschetti et al., 2025). In the latter hypothesis, Provence forms a rather small emerged continental domain between two Cretaceous rift segments.

The analyses of Raman Spectroscopy of Carbonaceous Material (RSCM) temperatures from the Digne Nappe, in the eastern part of the Vocontian basin (Fig. 2A), supports a tectonic model in which the Vocontian basin resulted from two superimposed phases of crustal thinning. The first one is dated to the Upper Jurassic and coincides with the Alpine Tethys opening. The second phase, characterised by temperatures in the basin exceeding 300°C, is believed to have occurred during the Lower Cretaceous period, when the Pyrenean rifting led to continental breakup in the Valaisan domain (Célini et al., 2023).

Despite the well-established structural and sedimentary constraints on the tectonic evolution of the basin, including clear evidence for syn-depositional normal faulting in the mid-Cretaceous

https://doi.org/10.5194/egusphere-2025-3332
Preprint. Discussion started: 28 July 2025

(e.g., Homberg et al., 2013), precise geochronological constraints on the timing of rifting and subsequent inversion are lacking. Resolving this question is critical, as the timing of the end of Cretaceous extension often overlaps with the onset of Pyrenean compression (Bilau et al., 2023). Furthermore, it is unclear whether this part of the Alpine foreland experienced the same extension associated as the West European Rift, as seen in the Valence and Manosque basins (e.g., Ford and Lickorish, 2004).

This study addresses these questions through an approach combining U-Pb dating of calcite in faults and veins complemented with new RSCM thermochronology and analysis of the burial history of the Vocontian basin. We aim to clarify the interactions between the different tectonic systems that developed in SE France by establishing a robust chronological framework. Our findings have significant implications for our understanding of polyphase deformation at the Europe-Iberia-Adria plate boundary.

2. Geological setting

Positioned at the front of the Western Alps, the Vocontian Basin is part of the Southern Subalpine belt produced by the interactions between the Pyrenean-Provençal belt to the south and the Alpine belt to the east (Philippe et al., 1998; Balansa et al., 2022; Célini et al., 2024; Fig. 1). It includes the Diois-Baronnies region, and it is bordered by the Rhône Valley and the Massif Central basement to the west, the External Crystalline Massif of Pelvoux to the east, the Vercors Massif to the north, and the Provençal Platform to the south (Figs. 1, 2A).

The Vocontian Basin is filled by approximately 2,600 m thick succession of mostly Mesozoic deposits along its margins reaching a thickness of up to 7,000 m in its center (Fig. 2B).

The base of the folded stratigraphic sequence is made of upper Triassic evaporites which have led to the development of salt diapirs piercing the sedimentary cover (Suzette, Propiac diapirs), or controlling certain features of the basin including thickness variations (Fig. 3A) (Célini, 2020 and references therein).

The subsidence at the origin of the basin initiated with the opening of the Alpine Tethys to the east during the Early to Middle Jurassic. This period is marked by the deposition of alternating shallow marine limestones and marls, followed by deepening marine environments culminating with the deposition of organic-rich black shales of the “Terres Noires” formation during the Bathonian–Oxfordian (Fig. 2). In the Late Jurassic, the basin underwent NNE–SSW-directed extension, as recorded by syn-sedimentary NNW–SSE-trending normal faults (Homberg et al., 2013). This extensional regime, consistent with the propagation of the Alpine Tethys, led to the deposition of fine-grained bioclastic Tithonian Limestones, which form a distinctive

https://doi.org/10.5194/egusphere-2025-3332
Preprint. Discussion started: 28 July 2025

morphostructural marker and reflect slower subsidence (Remane, 1970; Joseph et al., 1988). The subsidence continued throughout the Early Cretaceous (Valanginian-Aptian) period, during which alternating layers of marls and limestones were deposited, shaping the "Vocontian facies". These deeper marine deposits contrast with the shallow-water carbonates of the Vercors platform to the north, known as the "Urgonian facies" (Fig. 2A).

A major shift in tectonic regime occurred during the Aptian–Albian, marked by increased subsidence and the deposition of thick marly sequences ("Blue Marls"; Debrand-Passard et al., 1988) (Fig. 2B). This phase is associated with the development of E–W-trending normal faults, suggesting a reorientation of the extensional stress field from NNE–SSW (Late Jurassic) to WNW–ESE (Homberg et al., 2013). This shift is interpreted to reflect plate tectonic reorganization, linked to the onset of Europe–Iberia divergence (Bay of Biscay opening) and the closure of the Alpine Tethys through Europe-Adria convergence (Lemoine et al., 1987; Stämpfli, 1993).

During the Late Cretaceous, sandstones were deposited in the west whereas limestones predominated in the east of the basin (Fig. 2). At the current location of the Dévoluy massif, in the north-eastern part of the basin, a stratigraphic hiatus of the Turonian, Coniacian to the Santonian (Fig. 3B) is documented, regionally referred to as the Turonian unconformity. It is marked by the argillaceous to sublithographic limestones of the lower Cretaceous and E-W trending folds which are in direct contact, below an erosional surface, with bioclastic and terrigenous deposits of the Campanian-Maastrichtian (Fig. 2-3B; Gidon et al., 1970; Arnaud et al., 1974). In the entire Vocontian basin the main stratigraphic hiatus corresponds to Paleocene-Early Eocene (Fig. 2B). This late Cretaceous-Paleocene is coeval with the onset of Iberia-Europe convergence, marking the initial stages of the Pyrenean-Provençal orogeny from ~84 Ma (Angrand and Mouthereau, 2021; Mouthereau et al., 2014; Muñoz, 1992; Teixell et al., 2018; Ford et al., 2022). These deformations are consistent with the exhumation at ~85 Ma of the Pelvoux crystalline basement to the northeast (Fig. 2; Boschetti et al., 2025).

After this tectonic change, only limited and localized marine incursions occurred from the Late Eocene to the Miocene (Fig. 2B). This period corresponds to the early Alpine collision, which affected the internal domains and the eastern parts of the External Crystalline Massifs. Meanwhile, regional-scale extension developed in the European plate due to the evolution of the Western European Rift system and the opening of the Liguro–Provençal back-arc basin in southeastern France (Fig. 1) (Hippolyte et al., 1993; Séranne et al., 2021; Jolivet et al., 2021).

In the eastern part of the basin, the latest compressional phase is recorded by N–S to NW–SE-trending structures associated with the Digne thrust (Fig. 1-2) and final Alpine exhumation between ~12 and 6 Ma (Schwartz et al., 2017).

3. Sampling and methods

3.1 Sampling strategy

The sampling sites were carefully selected to characterize both the nature and ages of the brittle deformation that affected the Jurassic and Cretaceous formations within the Vocontian basin (Fig. 2A). The main structures were first identified based on the work of Homberg et al. (2013), who described syn-extensional features in the Vocontian Basin that were formed "shortly after" sediment deposition. We used the 1:50.000 scale geological maps from Die to Sisteron to select our sampling targets.

3.2 Tectonic and paleostress analysis

To reconstruct the tectonic evolution of brittle deformation in the Vocontian Basin, fault-slip data and other stress indicators like calcite veins, were measured in the field and collected for U-Pb dating. Local stress states were inferred by inverting fault slip data using the methodology outlined by Angelier (1990), implemented in the Win-Tensor software (Delvaux and Sperner, 2003). This analysis provided the orientation of the three principal stress axes (σ1, σ2, and σ3) and the shape of the stress ellipsoids defined by the ratio $\phi = \frac{\sigma 2-\sigma 3}{\sigma 1-\sigma 3}$, reflecting the relative magnitudes of the principal stresses. Relative chronology between the reconstructed stress tensors was achieved through cross-cutting relationships between generations of veins and faults (normal, reverse, or strike-slip faults). Chronology with respect to folding was further refined by comparing the orientation of faults, veins, and/or associated stress states in their present-day configuration and after unfolding. This approach assumes that faults were neoformed according to an Andersonian state of stress, with one principal stress axis being vertical.

3.3 Calcite U-Pb geochronology

Prior to U-Pb analyses, each polished thick section was petrographically characterized at IPRA (Institut Pluridisciplinaire de Recherche Appliquée) in Pau, France. This characterization involved the use of an optical microscope coupled with cathodoluminescence (CL) imaging to identify multiple calcite generations. CL images were acquired using an OPEA Cathodyne system coupled with a Nikon BH2 microscope, operating at an acceleration voltage of 12.5 kV and an intensity of 300–500 mA. The U-Pb absolute dating of calcite was performed at IPREM (Institut des Sciences Analytiques et de Physico-Chimie pour l'Environnement et les Matériaux) laboratory, following the analytical approach described by Hoareau et al. (2021). This method employs isotopic mapping of U, Pb, and Th via a continuous ablation process, combined with a virtual spot method to construct Tera-Wasserburg (TW) plots (Hoareau et al., 2021, 2024). A comprehensive description of the analytical procedure and data processing is provided in the Supplementary Material 1 (Tab. A1, Tab. A2). The analytical setup included a 257 nm femtosecond laser ablation system (Lambda3, Nexeya, Bordeaux, France), operating at a frequency of 500 Hz with a spot size of 15 µm. Ablation was conducted in a controlled atmosphere composed of helium (600 mL/min) and nitrogen (10 mL/min), which was subsequently mixed with argon in the ICPMS. This system was coupled to an HR-ICPMS Element XR (ThermoFisher Scientific, Bremen, Germany) equipped with a jet interface (Donard et al., 2015).

3.4 Burial history

The subsidence history of the Vocontian Basin was reconstructed using stratigraphic sections including thicknesses and lithologies, from the 1:50.000 scale geological maps of Die, Mens, Dieulefit, Luc-en-Diois, Gap, Nyons, Serres, Laragne-Montéglin, Vaison-la-Romaine, and Séderon, providing basin-wide coverage (Fig. 4). Standard backstripping techniques (Allen and Allen 2013) were applied for this analysis. The sedimentary units were first decompacted using a coefficient corresponding to the main lithology (limestone, marl or clay) and stratigraphic ages inferred from the geological maps. To enable comparison between the different sedimentary columns, the stratigraphic columns were resampled at regular temporal intervals, every 1 Myr, grouped into bins of 5 Myr and finally interpolated using the 2D spline method.

3.5 RSCM thermometry approach

To determine the peak temperatures reached by sediments and metasediments in the Vocontian basin, we conducted RSCM analyses on an initial set of rock samples collected from Middle to Upper Jurassic and Lower Cretaceous carbonates close to U-Pb dated calcites (Fig. 2A, 4). For comparison, this set was complemented by a second set of samples further eastwards in, or near, the Authon-Valavoire thrust nappe (below the Digne nappe) where deeper Lower Jurassic strata of the Vocontian are exposed and diapirism has been described (e.g., Célini et al., 2024). The RSCM approach is used to understand thermal processes ranging from advanced diagenesis to high-grade metamorphism, covering temperatures from 100 to 650°C (e.g., Ayoa et al., 2010; Koukestu et al., 2014; Schito et al., 2017). Depending on the temperature range and the geological context, different calibrations are proposed. In this study, we applied the calibration of Lahfid et al. (2010) for temperatures ranging between 200 and 340°C, and the qualitative approach proposed in Saspiturry et al. (2020) for lower temperatures between 100 and 200°C. The analyses were performed at the Bureau de Recherches Géologiques et Minières (BRGM; Orléans, France). The Raman spectra were obtained with a Horiba LABRAM HR instrument with a 514.5 nm solid-state laser source for excitation. The laser is focused on the samples with a BxFM microscope using a x100 objective with a numerical aperture of 0.90 and under 0.1 mW on the sample surface.

4. Results

4.1 Microtectonics and paleostress reconstructions

Veins and striated planes associated with folds (Fig. 5A), reverse faults (Fig. 5B) and normal faults (Fig. 5C) were measured and sampled. Stereodiagrams of beddings, fault-slip data, veins and, when necessary, their associated back-tilting state of stress, are presented in Figure 6. When the number of fault-slip data was sufficient for inversion (a minimum of four is required), the calculated stress axes have been reported (Fig. 6; Table 1). In this section we first present data from samples VOC-23-09a to VOC-23-16d (in numerical order) and then introduces samples BON-23-01, 02, and 03, along with GLAN-23-02, which belong to a second and separate field campaign. No measurements were conducted for sample VOC-23-01a and VOC-23-01b, as the sampling area is located within a diapiric structure of the Dentelles de Montmirail (Figs. 2A, 6), preventing a reliable interpretation of the paleostress tensor.

The sampling area of sample VOC-23-09b shows a majority of strike-slip faults, for which paleostress inversion reveals a strike-slip regime resolving a NW-SE-directed compression (Fig. 6). At site of sample VOC-23-11a bedding is flat. We resolve a strike-slip regime with paleostress reconstructions that indicate a NE-SW compression and NW-SE extension (Figs. 5B, 6).

Samples VOC-23-12a and VOC-23-12b exhibit distinct deformation patterns. While sample VOC-23-12a corresponds to calcite veins consistent with WNW-ESE extension, sample VOC-23-12b exhibits similar calcite veins, as well as additional strike-slip deformation, as reported on the stereogram. This reflects WNW-ESE compression and NNE-SSW extension (Fig. 6), which is not significantly different from our result in sample VOC-23-09a and b site. The geometry of the stress axes, when considered alongside the dip and orientation of the bedding suggests that this state of stress occurred after folding.

Sample VOC-23-13 site shows strike-slip faults that are consistent with an E-W-directed extension and N-S-directed compression (Figs. 5C,6). Sample VOC-23-14a represents a calcite vein associated with sample VOC-23-14b, which exhibits a strike-slip fault with a sinistral component. Paleostress reconstruction indicates a WNW-ESE extension and NNE-SSW compression (Fig. 6).

Sample VOC-23-16d shows calcite veins affected by strike-slip deformation. In contrast, sample VOC-23-12b only shows strike-slip deformation (post-vein) on the stereogram. Paleostress calculation indicates an NW-SE-directed extension (Fig. 6). Samples BON-23-01a and BON-23-01b correspond to a striated calcite that has been affected by layer-parallel shortening (LPS). This is interpreted as representing flexural slip during folding (Lacombe et al., 2021) (Figs. 5A, 6). Sample BON-23-01c is a calcite vein that formed within the same fold as the previous samples. It is interpreted to have formed during the growth of the fold. Paleostress analysis of the Bonneval outcrop indicates N20°E compression associated with the formation of the N110°E fold (Figs. 5A, 6). Finally, the GLAN-23-02 sample outcrop exhibits a normal fault coherent with a NE-SW extension direction.

4.2 Petrography of calcite samples

In summary, 15 samples were dated in this study: 6 veins (samples VOC-23-01a, 01b, 09b, 12a, 14b and BON-23-03) and 9 fault planes with striations (samples VOC-23-9a, 11a, 12b, 13, 14a, 16d, BON-23-01, 02 and GLAN-23-02). Most samples exhibit millimetric to centimetric blocky or elongate-blocky calcite (Fig. 5) (samples VOC-23-01, 9a, 12a, 22b, 13a, 14a, BON-23-01, 02, 03 and GLAN-23-02). They are characterized by homogeneous luminescence, indicating no evidence of multi-phase calcite growth (Figs. 7A, B). Two samples exhibit different calcite morphologies. Sample VOC-23-11a contains a centimetric calcite with a transitional morphology between syntaxial and stretching (Figs. 7C, D). This suggests the presence of crystals with variable growth planes within the fault plane, indicating potential multiple crack-seal events. Similarly, sample VOC-23-16d displays millimetric to centimetric calcite, predominantly composed of blocky calcite, which appears to be crosscut by a more elongated and stretched second calcite generation (Fig. 7C, D).

4.3 Calcite U-Pb geochronology

This study presents 16 new calcite U-Pb ages from eight types of brittle structures (Table 1; Figs. 8, 9, 10). The Tera-Wasserburg diagrams show data well spread along the discordia line. The Mean Squared Weighted Deviation (MSWD) ranges from 1.1 to 1.9, which is consistent with well-resolved age estimates. Three distinct age groups can be identified from this dataset. The first age group corresponds to the Late Cretaceous to Early Eocene periods from veins collected in late Jurassic-Early Cretaceous strata in the West. Ages obtained in the "Dentelles de Montmirail" area are of 82.9 ± 3.8 Ma (sample VOC-23-01b) and 76.5 ± 3.4 Ma (sample VOC-23-01a). To the North of the study area, in the Die region, corresponding fold structures associated with N20°E shortening are dated to 72.0 ± 3.7 Ma (sample BON-23-01a), 71.2 ± 8.1 Ma (sample BON-23-01b), and 50.0 ± 4.3 Ma (sample BON-23-01c) (Fig. 8).

The second age group corresponds to veins and faults dated back to the Oligocene. Obtained ages range from 34.3 ± 1.5 Ma (vein: VOC.23.14a), 30.3 ± 1.5 Ma (fault: VOC.23.14b2), 30.0 ± 2.8 Ma (fault: VOC.23.13b), 28.1 ± 1.2 Ma (fault: VOC.23.14b1), 25.6 ± 1.3 Ma (vein: VOC.23.12a), 23.2 ± 1.3 Ma (deformed vein: VOC.23.12a and b) and 27.6 ± 5.4 Ma (fault: GLAN.23.02) (Fig. 9). Most of these fractures correspond to NW-SE to NE-SW extension (Fig. 6). One of them, sample VOC.23.12b, which is the same kind of veins as VOC.23.12a, is consistent with a strike-slip regime with NNE-SSW extension and WNW-ESE compression similar to sample VOC.23.09 (Fig. 6).

The third age group corresponds to Miocene veins and strike-slip faults collected in Upper Jurassic-lower Cretaceous carbonates. Two subgroups can be distinguished. The first subgroup, characterized by ages of 12.2 ± 3.2 Ma and 12.5 ± 5.2 Ma (fault: VOC.23.11a and fault: VOC.23.16d), is associated with a strike-slip regime consistent with NE-SW compression and NW-SE extension (Figs. 10, 6). The second subgroup, defined by ages of 7.8 ± 0.6 Ma and 7.0 ± 2.2 Ma (fault: VOC.23.09a and vein: VOC.23.09b) also corresponds to a strike-slip regime but corresponds to NW-SE compression and NE-SW extension (Figs. 10, 6).

4.5 RSCM thermometry

RSCM data from the first set of Upper Jurassic and Lower Cretaceous carbonates in the central and southern parts of the studied area indicate that temperatures did not exceed 100°C (samples VOC-23-01 and VOC-23-16; Table 2). For the second set of samples, temperatures were successfully determined for 12 samples using an appropriate calibration (Table 2, Fig. 6), which can be divided in two subgroups. Temperatures measured in Lower to Upper Jurassic strata sampled near Saint Roman and Montmaure in the Die area display the lowest temperatures ranging between 100 and 180°C (samples VOC-18-17, VOC-18-18), near Veynes and close to the Devoluy massif (sample VOC-18-20), Sigoyer village (samples VOC-18-21, VOC-18-22), and in the upper stratigraphic unit of the Authon-Valavoire nappe (sample VOC-18-28), in the eastern of the basin, below this nappe (sample VOC-18-29). The higher bound of RSCM temperatures at 170°C is measured for samples VOC-18-24a and 33 located near diapiric structures: “Rocher de Hongrie” (Célini et al., 2024). The latter values are consistent with temperatures between 140 and 200°C recently published in the vicinity of this diapir (Célini et al., 2024). The second subgroup defined by temperatures between 215 and 275°C are found 1 km to the south of Sigoyer (sample VOC-18-23), in the middle Jurassic layers in the hangingwall of the Authon-Valavoire nappe (sample VOC-18-25) and in the Lias strata near the Astoin diapir (VOC-18-31). Temperatures of this second subgroup fall within the temperature range recorded in the Authon-Valavoire nappe, closer to the Digne nappe, near Astoin (Célini et al., 2024). To summarize, our data reveal a thermal contrast between the western and eastern domains of the Vocontian basin. While the organic matter of upper Jurassic-lower Cretaceous formations is thermally immature, deeper Early-Middle-Late Jurassic formations exposed in the eastern part of the Vocontian basin, close to the Authon-Vallavoire and Digne nappes show significantly higher thermal maturity with RSCM temperatures exceeding 180°C and reaching up to 275°C. The shift towards higher RSCM temperatures between the Upper Jurassic-Early Cretaceous and deeper stratigraphic units of the Early-Middle Jurassic has also been observed in stratigraphic columns analysed from the Digne Nappe (Célini et al., 2022; Balansa et al., 2023).

4.4 Burial histories and temperatures reached in the basin

Burial histories for the Vocontian Basin are presented in Figure 11. Each curve represents burial evolution calculated from a synthesis of stratigraphic thicknesses inferred from the BRGM 1/50.000 geological maps covering the basin. A first observation is that the total sediment accumulation in the Vocontian basin appears to have reached a maximum of 6-7 km since the Early Jurassic. This is shown by the decompacted thicknesses of 6800 m in the Die region, or 5900 m in Nyons, in the northern and western parts of the basin, respectively. In regions of the basin where the lower Jurassic series are not exposed the total subsidence is obviously lower; it is only 2500 m in the region of Vaison-la-Romaine. Despite these differences, most regions recorded a main phase of burial during the Middle Jurassic, in the Callovian, about 160 Ma (Fig. 11). This phase affected the entire Vocontian Basin. It is shown by the deposition of marl to shale deposits of the “Terres Noires” facies characteristic of the External Alps. During this period about 2 km of “Terres Noires” were deposited (accumulation of 200-400 m/Myr). After

https://doi.org/10.5194/egusphere-2025-3332
Preprint. Discussion started: 28 July 2025

the Middle Jurassic, the burial slowed down but continued throughout the Late Jurassic and Early Cretaceous. A second phase of accelerated subsidence took place during the Early Cretaceous, around 130 Ma, in the Hauterivian. It is documented in the Mens section by the deposition of about 700 m of marls and limestones (Fig. 4). A third main phase of burial is recorded around 100-90 Ma (Fig. 11) in 6 out 10 stratigraphic sections. It is characterized by increasing siliciclastic influx revealed by the deposition of sandstones alternating with marls and limestones with a thickness of about 700-800 m (e.g., Nyons, Sédéron, Vaison-la-Romaine) (Fig. 10). The Gap, Laragne-Montéglin, and Mens sections, however, record erosion rather than sedimentation at this time. These depositional patterns reveal both uplift in the source regions and structural compartmentalization in the Vocontian basin (Fig. 11). A last episode of subsidence of maximum 350-500 m (e.g., Die, Laragne) is documented during the Eocene-Oligocene (Fig. 11).

5. Discussion

5.1 The Vocontian basin at the time of Mesozoic rifting: E-W trend in thermal gradients and low Ca-rich fluid circulation

The Vocontian basin recorded a prolonged phase of subsidence during the Jurassic and Cretaceous (Fig. 11), which is however not associated with a distinct fluid event. This period coincides with the rifting of the European paleomargin as inferred by the thermal evolution of the Variscan crystalline basement of the Pelvoux massif (Boschetti et al., 2025) to the North, and burial history below the Digne Nappe (Célini et al., 2023), which bounds the Vocontian to the east. This latter Eastern rim of the basin was likely inverted during the late stages of the Alpine collision between 12 and 6 Ma (Schwartz et al., 2017). We distinguish a first major phase of sedimentary burial that occurred during the Callovian-Oxfordian, between 170 and 160 Ma. It postdates the necking of the European paleomargin as identified in the External Crystalline Massifs (Mohn et al., 2014; Ribes et al., 2020; Dall'Asta et al., 2022) and is synchronous with the opening of the Alpine Tethys (Lemoine, 1987; Manatschal and Müntener, 2009). It is recognized in the Vocontian basin, where it is expressed by WNW–ESE extension across the entire basin (Dardeau et al., 1988; Homberg et al., 2013), but it is not recorded in our calcite U-Pb ages. Similar observations can be made for the subsequent extensional Cretaceous event at around 135 Ma, for which no fault of that age is reported. The high temperature measured in the Vocontian basin of the Digne Nappe at this time are interpreted to reflect renewed extension in the basin as the Valaisan domain opened along the European margin (Célini et al., 2023), consistent with continuous burial heating recorded in the Pelvoux massif

(Boschetti et al, 2025). This new peak in sedimentation is consistent with a shift from the Middle Jurassic WNW–ESE extension to NNE–SSW extensional regime during the Barremian to Aptian interval (Dardeau, 1988; de Graciansky and Lemoine, 1988; Homberg et al., 2010). This later extensional event is recorded not only throughout the Vocontian Basin (Homberg et al., 2013), but also along its margins. Evidence includes deformation along the Ventoux–Lure fault zone (Beaudoin et al., 1986; Huang et al., 1988), the development of large-scale sliding domains on the Vercors platform (Bièvre and Quesne, 2004), and subsidence in E–W-oriented domains along the Ardèche margin during the same period (Cotillon et al., 1979). Our RSCM analyses show an increase of peak temperatures towards the East of the Vocontian where deeper Lower Jurassic stratigraphic series are exposed (Fig. 6; Table 2). When compared to burial temperature estimates ranging from normal (30°C/km) to high (60°C/km) geothermal gradients, we infer that our RSCM data reveal high to extreme gradients in the East, that is, in the direction of increasing crustal thinning in the Vocontian-Valaisan rift segment (Fig. 6; Table 2). Note that the sharp increase in the geothermal gradients is not necessarily entirely related to crustal thinning but also largely a response of mantle thinning and asthenosphere uprising. The lack of calcite mineralisation at this age in brittle tectonic features is intriguing. Indeed, evidence of mineralization of barite, authigenic quartz and pyrite in the Callovian-Oxfordian shales in the deeper part of the basin is interpreted as reflecting basal fluid flow during peak burial in the Middle Cretaceous, as well as brines related to salt diapirs (Guilhaumou et al., 1996). We suggest that the absence of Middle Cretaceous calcites can reflect the fact that 1) faulting occurred at a depth too shallow for calcite precipitation and/or 2) subsequent burial to depth of 2-3 km, in the East, led to the dissolution of previous Middle Cretaceous calcites in response to changing physical conditions (e.g., pH, temperature). In addition, mechanical decoupling in the Triassic salt layer during extension may have resulted in the localization of fluid flow and deformation at the base of the basin.

A third depositional phase occurred around 100-90 Ma, in agreement with syn-faulting deposits along the Clausis and Glandage fault systems in the Vocontian/Dévoluy basin (Fig. 11, 3) (Gidon et al., 1970; Arnaud et al., 1974) and strike-slip motions along the Toulourenc faults in the Ventoux-Lure massif (Montenat et al., 2004). On a broader scale, this tectonic phase coincides with strike-slip movements along the Cevennes, Nîmes and Durance faults (Montenat et al., 2004; Parizot et al., 2022), possibly associated with local compression related to diapiric movement at 95-90 Ma (Bilau et al., 2023) and normal faulting reported in Provence (Zeboudj et al., 2025). This episode is a response of the continental rifting between Iberia-Ebro and European plates, and the formation of the Pyrenean rift system (Angrand and Mouthereau,

https://doi.org/10.5194/egusphere-2025-3332
Preprint. Discussion started: 28 July 2025

2021) (Fig. 12A). Strike-slip movements along inherited faults (Cevennes, Nîmes, Durance faults) were associated with oblique extension accommodated by overlapping rift segments in the Pyrenean and Vocontian basins (Fig. 12). This complex tectonic setting likely triggered the emergence of continental blocks that can explain the abundance of sandstone deposits during this period in the Vocontian basin (Fig. 4, 11). This interpretation aligns with the documented formation of an uplifted structure in Provence during the Albian-Cenomanian, known as the Durancian Isthmus (Combes, 1990; Guyonnet-Benaize et al., 2010; Chanvry et al., 2020, Marchand et al., 2021). Cooling and exhumation in the Massif Central to the west are also documented from 120-90 Ma (Olivetti et al., 2016), which may have contributed to feeding of the Vocontian basin during this period (Fig. 12A). It should be reminded that the locally complex tectonic evolution of SE France during the Middle-Late Cretaceous is a response to large-scale differential movements between Iberia-Ebro and Adria that accommodated both extension in the Pyrenees-Provence rift and contraction in the Alps (e.g., Le Breton et al., 2021; Angrand and Mouthereau, 2021; Boschetti et al., 2025, In Press).

5.2 Post-Mid Cretaceous evolution of the Vocontian basin: U-Pb/calcite dating record of multiple collision and rifting events in the SE basins of France

The oldest calcite U-Pb ages of 84.6 ± 2.4 Ma and 77.7 ± 2.9 Ma reported in the Jurassic strata forming the wall of the Suzette diapir in the “Dentelles de Montmirail” structure are consistent with the age of the onset of the Pyrenees-Provence collision dated around 84 Ma (Angrand and Mouthereau, 2021; Mouthereau et al., 2014; Muñoz, 1992; Teixell et al., 2018; Ford et al., 2022). Those old calcite ages are likely to be realed to halokinetic movement of Suzette diapir in response to far-field stresses that trigger tectonic inversion and exhumation all over Europe (Mouthereau et al., 2021). These ages can also be related to folding along E-W trending folds in the Dévoluy massif, affecting the Early Cretaceous units and associated to erosional surface dated to Coniacian-Santonian (Fig. 3B) (ca. 85 Ma) (Flandrin, 1966; Lemoine, 1972; Gidon et al., 1970; Arnaud et al., 1974), or the end of diapiric movement during extension in southern Provence (Wicker and Ford, 2021). In the Pyrenees exhumation seems to increase from 75-70 Ma (Mouthereau et al., 2014) and this is recorded regionally in SE of France by the cooling of the Pelvoux to the Maures-Tanneron massifs (Fig. 12A) (Boschetti et al., 2025, In Press). This timing is further in line with the earliest surface deformation, which is recorded around 75 Ma (Parizot et al., 2021). U/Pb ages of 72.0 ± 3.7 Ma and 71.2 ± 8.1 Ma associated with folding during N20°E compression are consistent with the latest sinistral reactivation of the Cevennes fault from 76 Ma (Parizot et al., 2021). These ages can also be related to folding along E-W axis in the Dévoluy massif, affecting the Early Cretaceous units and associated to erosional surface estimated to occur during Turonian-Coniacian-Santonian (Fig. 3) (ca. 85 Ma) (Flandrin, 1966; Lemoine, 1972; Gidon et al., 1970; Arnaud et al., 1974).

Our data resolve another later N20°E contractional stage dated at 50.0 ± 4.3 (Fig. 6). It is well identified also in Provence in the U/Pb age dataset (Zeboudj et al., 2025) and correspond to a N-S compressive phase spanning from 59 to 34 Ma. This stage is regarded as the culmination of the Pyrenean-Provençal collision (Bestani et al., 2016; Balansa et al., 2022) (Fig. 12B). This episode is related to the acceleration of collision at ca. 50 Ma caused by dynamic changes in Africa motion, and North Altantic opening (e.g. Mouthereau et al., 2021). In northwestern Europe, the Eocene also announces the onset of opening of the aborted rift system of the West European Rift (WER) (e.g. Séranne et al., 1999; Dèzes et al., 2004; Mouthereau et al., 2021). The WER stage is well represented in the Vocontian basin as indicated by eight U/Pb dates ranging from 30.4 ± 2.7 to 24.3 ± 1.3 Ma (Fig. 12C), which coincides with an extensional phase (35–23 Ma) also documented in Provence, western Alps, eastern Pyrenees, and Valencia Trough, coeval with the late activities of the West European Rift (Merle and Michon, 2001; Ziegler and Dèzes, 2006). In our study region the shallow depth of iso-velocity contour Vs=4.2 $km.s^{-1}$, considered to be a proxy for the Moho (Schwartz et al., 2024), confirms a significant crustal thinning in the Valence-Rhone depression (Fig. S1, Supplementary Material 1). It should also be noted that the Late Eocene-Early Oligocene period coincided with the onset of deposition in the flexural basin of the Alpine foreland (Ford et al., 1999). The deflection of the European margin is likely increasing the extensional stresses associated with the WER. From Chattian-Aquitanian times, at ca. 23 Ma, the opening of the Gulf of Lions and of the Ligurian basin (e.g., Séranne et al., 1999; Jolivet et al., 1999, 2020) commenced following the demise of the WER (Mouthereau et al., 2021) (Fig. 12C). The excellent preservation of the Oligocene-Miocene extensional phase suggests positive feedbacks between crustal thinning (Fig. S1, Supplementary Material 1) and physical conditions become favourable to calcite precipitation closer to the surface, as the basin was exhumed during the former Late Cretaceous shortening. The youngest calcite U/Pb ages of 12.2 ± 3.2 Ma, 12.5 ± 5.2 Ma, 7.8 ± 0.6 Ma and 7.0 ± 2.2 Ma are associated with NE-SW compression. This result agrees with the westward propagation of the Alpine deformation front, which migrated forelandward from 15 to 7 Ma in the Vercors massif (Bilau et al., 2023) (Fig. 12D). This timing also coincides with the exhumation of Alpine external crystalline massifs, such as the Belledonne and Pelvoux massifs (e.g. Beucher et al., 2012; Girault et al., 2022; Boschetti et al., 2025).

https://doi.org/10.5194/egusphere-2025-3332
Preprint. Discussion started: 28 July 2025

CONCLUSION

The goal of this study was to provide a refined chronology of deformation in the Vocontian Basin using an integrated approach combining U-Pb calcite geochronology, RSCM thermometry, and subsidence analysis. First, this study highlights the absence of mid-Cretaceous syn-rift calcites associated with the opening of the Vocontian Basin. This is possibly related to dissolution during subsequent burial, or reflect the localization of fluid flow and strain in the basal Triassic salt layer during the mid-Cretaceous extension. The temporal distribution of dated brittle structures reveals three main deformation episodes: (1) Late Cretaceous to Paleocene calcite precipitation associated with Pyrenean-Provençal convergence and diapirism; (2) Oligocene extensional phases tied to the West European Rift opening; and (3) Miocene strike-slip reactivation and contraction linked to the Alpine orogeny. These events are superimposed onto a long-term subsidence history that records major burial phases during the Jurassic and Cretaceous. Thermal data from RSCM analyses delineate a sharp eastward increase in geothermal gradients, suggesting enhanced crustal thinning and/or diapiric activity in the eastern part of the basin. This work highlights the possible mismatch between the tectonic evolution of a region and the tectonic history inferred from calcite U–Pb dating, which is sensible to burial history and the physical conditions required to precipitate syn-deformation calcite.

Declaration of Competing Interest

The authors declare that they have no known competing financial interests or personal relationships that could have appeared to influence the work reported in this paper.

Availability of data material

The dataset(s) supporting the conclusions of this article is(are) available in Supplementary Material 1.

Acknowledgments

Authors would like to thank BRGM and the RGF program which allows the founding this project.

Author’s contribution

LB is the corresponding author who carried out the field investigation, analysis, interpretation and drafting of the manuscript. MP carried out the field investigations, analysis and review of the manuscript. FM carried out the filed investigation, interpretation, drafting a review of the manuscript. GH carried out the U-Pb analysis and review of the Manuscript. SS and YR carried out the field investigation and review of the manuscript. DB carried out interpretation and discussion and AL carried out analysis of Raman data.

Funding

This study was made possible thanks to ministerial funding from the SDU2E doctoral school at Toulouse University and by additional the funding by the RFG-Alps programme, coordinated by the BRGM.

References

Allen, P. A., & Allen, J. R.: Basin analysis: Principles and application to petroleum play assessment. John Wiley & Sons, 2013.

Angelier, J.: Inversion of field data in fault tectonics to obtain the regional stress—III. A new rapid direct inversion method by analytical means. Geophysical Journal International, 103(2), 363-376.https://doi.org/10.1111/j.1365-246X.1990.tb01777.x, 1990.

Angrand, P., & Mouthereau, F.: Evolution of the Alpine orogenic belts in the Western Mediterranean region as resolved by the kinematics of the Europe-Africa diffuse plate boundary. BSGF-Earth Sciences Bulletin, 192(1), 42. https://doi.org/10.1051/bsgf/2021031, 2021.

Arnaud H., Charollais J., Delamette M. & Portault B. : Crétacé supérieur. Chaînes subalpines. In: S. Debrand-Passard et al., Eds, Syn thèse géo lo gique du Sud-Est de la France. – Mém.BRGM, 125, 355-359, 1984.

Balansa, J., Espurt, N., Hippolyte, J. C., Philip, J., & Caritg, S.: Structural evolution of the superimposed Provençal and Subalpine fold-thrust belts (SE France). Earth-Science Reviews, 227, 103972. https://doi.org/10.1016/j.earscirev.2022.103972, 2022.

Balansa, J., Lahfid, A., Espurt, N., Hippolyte, J. C., Henry, P., Caritg, S., & Fasentieux, B.: Unraveling the eroded units of mountain belts using RSCM thermometry and cross-section balancing: example of the southwestern French Alps. International Journal of Earth Sciences, 112(2), 443-458. https://doi.org/10.1007/s00531-022-02257-3, 2023.

Bestani, L., Espurt, N., Lamarche, J., Bellier, O., & Hollender, F.: Reconstruction of the

https://doi.org/10.5194/egusphere-2025-3332
Preprint. Discussion started: 28 July 2025

Provence Chain evolution, southeastern France. Tectonics, 35(6), 1506-1525- https://doi.org/10.1002/2016TC004115, 2016.

Beaudoin, B., Friès, G., Joseph, P., Bouchet, R., & Cabrol, C. : Tectonique synsédimentaire crétacée à l'ouest de la Durance (S.-E. France). Comptes rendus de l'Académie des sciences. Série 2, Mécanique, Physique, Chimie, Sciences de l'univers, Sciences de la Terre, 303(8), 713-718, 1986.

Beucher, R., van der Beek, P., Braun, J., & Batt, G. E.: Exhumation and relief development in the Pelvoux and Dora-Maira massifs (Western Alps) assessed by spectral analysis and inversion of thermochronological age transects. Journal of Geophysical Research: Earth Surface, 117(F3). https://doi.org/10.1029/2011JF002240, 2012.

Bièvre, G., & Quesne, D.:Synsedimentary collapse on a carbonate platform margin μ (lower Barremian, southern Vercors, SE France). Geodiversitas, 26(2), 169-184, 2004.

Bilau, A., Rolland, Y., Dumont, T., Schwartz, S., Godeau, N., Guihou, A., & Deschamps, P., 2023. Early onset of Pyrenean collision (97–90 Ma) evidenced by U–Pb dating on calcite (Provence, SE France). Terra Nova, 35(5), 413-423. https://doi.org/10.1111/ter.12665, 2004

Boschetti, L., Mouthereau, F., Schwartz, S., Rolland, Y., Bernet, M., Balvay, M., ... & Lahfid, A.: Thermochronology of the western Alps (Pelvoux massif) reveals the longterm multiphase tectonic history of the European paleomargin. Tectonics, 44(2), e2024TC008498. https://doi.org/10.1029/2024TC008498, 2025

Boschetti, L., Rolland, Y., Mouthereau, F., Schwartz, S., Milesi, G., Munch, P., Bernet, M., Balvay, M., Thiéblemont, D., Bonno, M., Martin, C. Monié, P.: Thermochronology of the Maures-Tanneron crystalline basement: Insights for SW Europe Triassic to Miocene tectonic history. Swiss Journal of Geoscience. https://doi.org/10.1186/s00015-025-00485-8, In Press

Célini, N. : Le rôle des évaporites dans l’évolution tectonique du front alpin: le cas de la nappe de Digne (Doctoral dissertation, Université de Pau et des Pays de l'Adour), 2020.

Célini, N., Pichat, A., Mouthereau, F., Ringenbach, J. C., & Callot, J. P.: Along-strike variations of structural style in the external Western Alps (France): Review, insights from analogue models and the role of salt. Journal of Structural Geology, 105048. https://doi.org/10.1016/j.jsg.2023.105048, 2023.

Célini, N., Pichat, A., Mouthereau, F., Ringenbach, J. C., & Callot, J. P.: Along-strike variations of structural style in the external Western Alps (France): Review, insights from analogue models and the role of salt. Journal of Structural Geology, 179, 105048. https://doi.org/10.1016/j.jsg.2023.105048, 2024.

Chanvry, E., Marchand, E., Lopez, M., Séranne, M., Le Saout, G., & Vinches, M. : Tectonic and climate control on allochthonous bauxite deposition. Example from the mid-Cretaceous Villeveyrac basin, southern France. Sedimentary Geology, 407, 105727. https://doi.org/10.1016/j.sedgeo.2020.105727, 2020.

Combes, P. J. : Typologie, cadre géodynamique et genèse des bauxites françaises. Geodinamica Acta, 4(2), 91-109. https://doi.org/10.1080/09853111.1990.11105202, 1990.

Cotillon, P., Ferry, S., Busnardo, R., Lafarge, D., & Renaud, B.: Synthèse stratigraphique et paléogéographique sur les faciès urgoniens du Sud de l'Ardèche et du Nord du Gard (France SE). Geobios, 12, 121-139. https://doi.org/10.1016/S0016-6995(79)80055-8, 1979.

Dall'Asta, N., Hoareau, G., Manatschal, G., Centrella, S., Denèle, Y., Ribes, C., & Kalifi, A. : Structural and petrological characteristics of a Jurassic detachment fault from the Mont-Blanc massif (Col du Bonhomme area, France). Journal of Structural Geology, 159, 104593. https://doi.org/10.1016/j.jsg.2022.104593, 2022.

Dardeau, G., Atrops, F., Fortwengler, D., De Graciansky, P. C., & Marchand, D. : Jeux de blocs et tectonique distensive au Callovien et a l'Oxfordien dans le bassin du Sud-Est de la France. Bulletin de la Société géologique de France, 4(5), 771-777, 1988.

Debelmas, J. : La zone subbriançonnaise et la zone valaisanne savoyarde dans le cadre de la tectonique des plaques. Géologie Alpine, 77, 3-8, 1988, 2001.

Delvaux, D., & Sperner, B.: New aspects of tectonic stress inversion with reference to the TENSOR program. https://doi.org/10.1144/GSL.SP.2003.212.01.06, 2003.

Debrand-Passard, S. : Synthèse géologique du Sud-Est de la France (Vol. 1). Editions BRGM.de Graciansky, P.C., & Lemoine, Marcel., 1988. Early Cretaceous extensional tectonics in the xsouthwestern French Alps; a consequence of North-Atlantic rifting during Tethyan spreading. Bulletin de la Société géologique de France, 4(5), 733-737, 1984.

Dèzes, P., Schmid, S. M., & Ziegler, P. A. : Evolution of the European Cenozoic Rift System: interaction of the Alpine and Pyrenean orogens with their foreland lithosphere. Tectonophysics, 389(1-2), 1-33. https://doi.org/10.1016/j.tecto.2004.06.011, 2004.

Donard, A., Pottin, A. C., Pointurier, F., & Pécheyran, C.: Determination of relative rare

https://doi.org/10.5194/egusphere-2025-3332
Preprint. Discussion started: 28 July 2025

earth element distributions in very small quantities of uranium ore concentrates using femtosecond UV laser ablation–SF-ICP-MS coupling. Journal of Analytical Atomic Spectrometry, 30(12), 2420-2428, 2015.

Espurt, N., Angrand, P., Teixell, A., Labaume, P., Ford, M., de Saint Blanquat, M., & Chevrot, S. Crustal-scale balanced cross-section and restorations of the Central Pyrenean belt (Nestes-Cinca transect): Highlighting the structural control of Variscan belt and Permian-Mesozoic rift systems on mountain building. Tectonophysics, 764, 25-45. https://doi.org/10.1016/j.tecto.2019.04.026, 2019.

Flandrin, J. : Sur l'âge des principaux traits structuraux du Diois et des Baronnies. Bulletin de la Société géologique de France, 7(3), 376-386. https://doi.org/10.2113/gssgfbull.S7-VIII.3.376, 1966.

Ford, M., Lickorish, W.H. & Kusznir, N.J.: Tertiary foreland sedimentation in the southern Subalpine chains, SE France: a geodynamic analysis. Basin Research, 11, 315–336. https://doi.org/10.1046/j.1365-2117.1999.00103.x, 1999

Ford, M., & Lickorish, W. H.: Foreland basin evolution around the western Alpine Arc. https://doi.org/10.1144/GSL.SP.2004.221.01.04, 2004.

Ford, M., Masini, E., Vergés, J., Pik, R., Ternois, S., Léger, J., ... & Calassou, S.: Evolution of a low convergence collisional orogen: a review of Pyrenean orogenesis. BSGF-Earth Sciences Bulletin, 193(1), 19. https://doi.org/10.1051/bsgf/2022018, 2022.

Gidon, M., Arnaud, H., Pairis, J. L., AprAHAMIAN, J., & Uselle, J. P. : Les déformations tectoniques superposées du Dévoluy méridional (Hautes-Alpes). Géologie Alpine, 46, 87-110, 1970.

Girault, J. B., Bellahsen, N., Bernet, M., Pik, R., Loget, N., Lasseur, E., ... & Sonnet, M.: Exhumation of the Western Alpine collisional wedge: New thermochronological data. Tectonophysics, 822, 229155. https://doi.org/10.1016/j.tecto.2021.229155, 2022.

Guilhaumou, N., Touray, J. C., Perthuisot, V., & Roure, F., Palaeocirculation in the basin of southeastern France sub-alpine range: a synthesis from fluid inclusions studies. Marine and Petroleum Geology, 13(6), 695-706. https://doi.org/10.1016/0264-8172(95)00064-X. 1996.

Guyonnet-Benaize, C., Lamarche, J., Masse, J. P., Villeneuve, M., & Viseur, S. : 3D structural modelling of small-deformations in poly-phase faults pattern. Application to the Mid-Cretaceous Durance uplift, Provence (SE France). Journal of Geodynamics, 50(2), 81-93. https://doi.org/10.1016/j.jog.2010.03.003, 2010.

Hoareau, G., Claverie, F., Pecheyran, C., Barbotin, G., Perk, M., Beaudoin, N. E., ... & Rasbury,

E. T.: The virtual spot approach: a simple method for image U-Pb carbonate geochronology by high-repetition rate LA-ICP-MS. EGUsphere, 2024, 1-35. https://doi.org/10.5194/egusphere-2024-2366, 2024.

Hoareau, G., Claverie, F., Pecheyran, C., Paroissin, C., Grignard, P. A., Motte, G., ... & Girard, J. P.: Direct U–Pb dating of carbonates from micron-scale femtosecond laser ablation inductively coupled plasma mass spectrometry images using robust regression. Geochronology, 3(1), 67-87. https://doi.org/10.5194/ gchron-3-67-2021, 2021.

Homberg, C., Barrier, E., Mroueh, M., Muller, C., Hamdan, W., & Higazi, F.: Tectonic evolution of the central Levant domain (Lebanon) since Mesozoic time. https://doi.org/10.1144/SP341.12, 2010.

Homberg, C., Schnyder, J., & Benzaggagh, M.: Late Jurassic-Early Cretaceous faulting in the Southeastern French Basin: does it reflect a tectonic reorganization?. Bulletin de la Société géologique de France, 184(4-5), 501-514. https://doi.org/10.2113/gssgfbull.184.4-5.501, 2013.

Hippolyte, J. C., Angelier, J., Bergerat, F., Nury, D., & Guieu, G.: Tectonic-stratigraphic record of paleostress time changes in the Oligocene basins of the Provence, southern France. Tectonophysics, 226(1-4), 15-35. https://doi.org/10.1016/0040-1951(93)90108-V. 1993

Huang, Q., Geometry and tectonic significance of Albian sedimentary dykes in the Sisteron area, SE France, J. Struct. Geol., 10, 453–462, 1988.

Jolivet, L., Frizon de Lamotte, D., Mascle, A., & Séranne, M.: The Mediterranean basins: Tertiary extension within the Alpine orogen—An introduction. Geological Society, London, Special Publications, 156(1), 1-14. https://doi.org/10.1144/GSL.SP.1999.156.01.02, 1999

Jolivet, L., Menant, A., Roche, V., Le Pourhiet, L., Maillard, A., Augier, R., ... & Canva, A.: Transfer zones in Mediterranean back-arc regions and tear faults. Bulletin de la Société Géologique de France, 192(1). https://doi.org/10.1051/bsgf/2021006, 2021.

Joseph, P., Beaudoin, B., Sempere, T., & Maillart, J. : Vallées sous-marines et systèmes d'épandages carbonatés du Berriasien vocontien (Alpes méridionales françaises). Bull. Soc. Geol. Fr, 8, 363-374, 1988.

Kouketsu, Y., Mizukami, T., Mori, H., Endo, S., Aoya, M., Hara, H., ... & Wallis, S.: A new approach to develop the R aman carbonaceous material geothermometer for low-grade metamorphism using peak width. Island Arc, 23(1), 33-50. https://doi.org/10.1111/iar.12057, 2014.

https://doi.org/10.5194/egusphere-2025-3332
Preprint. Discussion started: 28 July 2025

Lacombe, O., Parlangeau, C., Beaudoin, N. E., & Amrouch, K. : Calcite twin formation, measurement and use as stress–strain indicators: a review of progress over the last decade. Geosciences, 11(11), 445. https://doi.org/10.3390/geosciences11110445, 2021.

Lahfid, A., Beyssac, O., Deville, E., Negro, F., Chopin, C., & Goffé, B. (2010). Evolution of the Raman spectrum of carbonaceous material in low-grade metasediments of the Glarus Alps (Switzerland). Terra nova, 22(5), 354-360. https://doi.org/10.1111/j.1365-3121.2010.00956.x, 2010.

Le Breton, E., Brune, S., Ustaszewski, K., Zahirovic, S., Seton, M., & Müller, R. D. : Kinematics and extent of the Piemont–Liguria Basin–implications for subduction processes in the Alps. Solid Earth, 12(4), 885-913. https://doi.org/10.5194/se-12-885-2021, 2021.

Lemoine, M. : Rythme et modalités des plissements superposés dans les chaînes subalpines méridionales des Alpes occidentales françaises. Geologische Rundschau, 61, 975-1010. https://doi.org/10.1007/BF01820902, 1972.

Lemoine, M., Tricart, P. and Boillot, G.: Ultramafic and gabbroic ocean floor of the Ligurian Tethys (Alps, Corsica, Apennines): in search for a genetic model. Geology, 15: 622-625, 1987.

Manatschal, G., & Müntener, O.: A type sequence across an ancient magma-poor ocean–continent transition: the example of the western Alpine Tethys ophiolites. Tectonophysics, 473(1-2), 4-19. https://doi.org/10.1016/j.tecto.2008.07.021, 2009

Marchand, E., Séranne, M., Bruguier, O., & Vinches, M. : LA-ICP-MS dating of detrital zircon grains from the Cretaceous allochthonous bauxites of Languedoc (south of France): Provenance and geodynamic consequences. Basin Research, 33(1), 270-290. https://doi.org/10.1111/bre.12465, 2021.

Merle, O., & Michon, L.: The formation of the West European Rift; a new model as exemplified by the Massif Central area. Bulletin de la Societé géologique de France, 172(2), 213-221. https://doi.org/10.2113/172.2.213, 2021.

Mohn, G., Manatschal, G., Beltrando, M., & Haupert, I.: The role of rift-inherited hyper-extension in Alpine-type orogens. Terra Nova, 26(5), 347-353. https://doi.org/10.1111/ter.12104, 2014.

Montenat, C., Janin, M. C., & Barrier, P. : L'accident du Toulourenc: une limite Tectonique entre la plate-forme provençale et le Bassin vocontien à l'Aptien–Albien (SE France). Comptes rendus. Géoscience, 336(14), 1301-1310, 2004.

Mouthereau, F., Filleaudeau, P. Y., Vacherat, A., Pik, R., Lacombe, O., Fellin, M. G., ... &

Masini, E.: Placing limits to shortening evolution in the Pyrenees: Role of margin architecture and implications for the Iberia/Europe convergence. Tectonics, 33(12), 2283-2314. https://doi.org/10.1002/2014TC003663, 2014.

Mouthereau, F., Angrand, P., Jourdon, A., Ternois, S., Fillon, C., Calassou, S., ... & Baudin, T.: Cenozoic mountain building and topographic evolution in Western Europe: impact of billions of years of lithosphere evolution and plate kinematics. BSGF-Earth Sciences Bulletin, 192(1), 56. https://doi.org/10.1051/bsgf/2021040, 2021.

Muñoz, J. A.: Evolution of a continental collision belt: ECORS-Pyrenees crustal balanced cross-section. In Thrust tectonics (pp. 235-246). Dordrecht: Springer Netherlands, 1992.

Olivetti, V., Godard, V., Bellier, O., & Aster Team.: Cenozoic rejuvenation events of Massif Central topography (France): Insights from cosmogenic denudation rates and river profiles. Earth and Planetary Science Letters, 444, 179-191. https://doi.org/10.1016/j.epsl.2016.03.049, 2016.

Parizot, O., Missenard, Y., Haurine, F., Blaise, T., Barbarand, J., Benedicto, A., & Sarda, P.: When did the Pyrenean shortening end? Insight from U–Pb geochronology of syn-faulting calcite (Corbières area, France). Terra nova, 33(6), 551-559. https://doi.org/10.1111/ter.12547, 2021.

Parizot, O., Missenard, Y., Barbarand, J., Blaise, T., Benedicto, A., Haurine, F., & Sarda, P.: How sensitive are intraplate inherited structures? Insight from the Cévennes Fault System (Languedoc, SE France). Geological Magazine, 159(11-12), 2082-2094. https://doi.org/10.1017/S0016756822000152, 2022.

Ribes, C., Ghienne, J. F., Manatschal, G., Dall'Asta, N., Stockli, D. F., Galster, F., ... & Karner, G. D.: The Grès Singuliers of the Mont Blanc region (France and Switzerland): stratigraphic response to rifting and crustal necking in the Alpine Tethys. International Journal of Earth Sciences, 109, 2325-2352. https://doi.org/10.1007/s00531-020-01902-z, 2020.

Roure, F., Brun, J. P., Colletta, B., & Van Den Driessche, J.: Geometry and kinematics of extensional structures in the Alpine foreland basin of southeastern France. Journal of Structural Geology, 14(5), 503-519. https://doi.org/10.1016/0191-8141(92)90153-N, 1992.

Saspiturry, N., Lahfid, A., Baudin, T., Guillou-Frottier, L., Razin, P., Issautier, B., ... & Corre, B.: Paleogeothermal gradients across an inverted hyperextended rift system: Example of the Mauléon Fossil Rift (Western Pyrenees). Tectonics, 39(10), e2020TC006206. https://doi.org/10.1029/2020TC006206, 2020.

Schito, A., Romano, C., Corrado, S., Grigo, D., & Poe, B.: Diagenetic thermal evolution of organic matter by Raman spectroscopy. Organic Geochemistry, 106, 57-67. https://doi.org/10.1016/j.orggeochem.2016.12.006, 2017.

Schwartz, S., Gautheron, C., Audin, L., Dumont, T., Nomade, J., Barbarand, J., ... & van der Beek, P.: Foreland exhumation controlled by crustal thickening in the Western Alps. Geology, 45(2), 139-142, 2017

Schwartz, S., Rolland, Y., Nouibat, A., Boschetti, L., Bienveignant, D., Dumont, T., ... & Mouthereau, F.: Role of mantle indentation in collisional deformation evidenced by deep geophysical imaging of Western Alps. Communications Earth & Environment, 5(1), 17. https://doi.org/10.1038/s43247-023-01180-y, 2024.

Séranne, M.: The Gulf of Lion continental margin (NW Mediterranean) revisited by IBS: an overview. Geological Society, London, Special Publications, 156(1), 15-36. https://doi.org/10.1144/GSL.SP.1999.156.01.03, 1999.

Séranne, M., Couëffé, R., Husson, E., Baral, C., & Villard, J. : The transition from Pyrenean shortening to Gulf of Lion rifting in Languedoc (South France)–A tectonic-sedimentation analysis. BSGF-Earth Sciences Bulletin, 192(1), 27, 2021.

Teixell, A., Labaume, P., Ayarza, P., Espurt, N., de Saint Blanquat, M., & Lagabrielle, Y.: Crustal structure and evolution of the Pyrenean-Cantabrian belt: A review and new interpretations from recent concepts and data. Tectonophysics, 724, 146-170. https://doi.org/10.1016/j.tecto.2018.01.009, 2018.

Trümpy, R.: A possible Jurassic-Cretaceous transform system in the Alps and the Carpathians. https://doi.org/10.1130/SPE218-p93, 1988.

Turco, E., Macchiavelli, C., Mazzoli, S., Schettino, A., & Pierantoni, P. P. : Kinematic evolution of Alpine Corsica in the framework of Mediterranean mountain belts. Tectonophysics, 579, 193-206, 2012.

Wicker, V., & Ford, M.: Assessment of the tectonic role of the Triassic evaporites in the North Toulon fold-thrust belt. BSGF-Earth Sciences Bulletin, 192(1), 51. https://doi.org/10.1051/bsgf/2021033, 2021.

Zeboudj, A., Lacombe, O., Beaudoin, N. E., Callot, J. P., Lamarche, J., Guihou, A., & Hoareau, G.: Sequence, duration, rate of deformation and paleostress evolution during fold development: Insights from fractures, calcite twins and U-Pb calcite geochronology in the Mirabeau anticline (SE France). Journal of Structural Geology, 105460. https://doi.org/10.1016/j.jsg.2025.105460, 2025.

Ziegler, P. A., & Dèzes, P.: Crustal evolution of western and central Europe. https://doi.org/10.1144/GSL.MEM.2006.032.01.03, 2006.

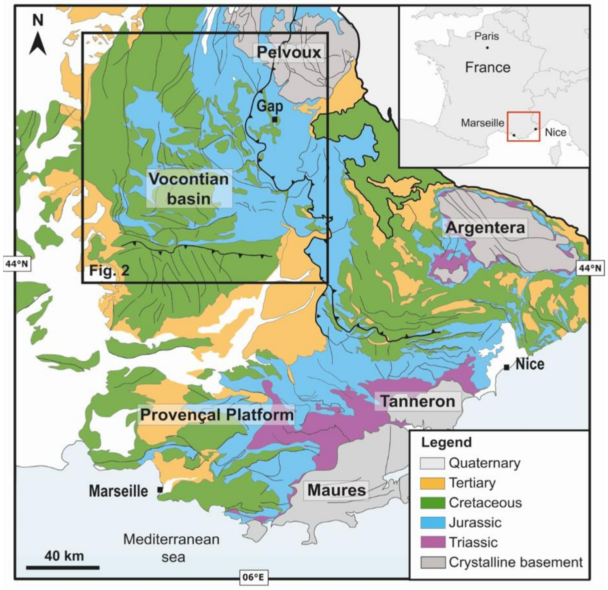

Figure 1: Simplified geological map of SE France. Location of the study area.

https://doi.org/10.5194/egusphere-2025-3332
Preprint. Discussion started: 28 July 2025

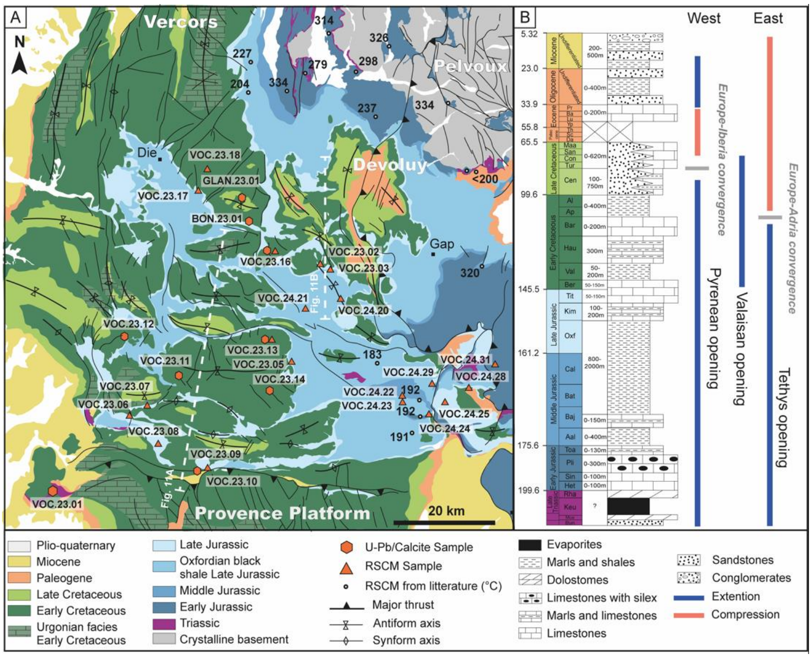

Figure 2: A) Geological map of Vocontian basin with sample location and Raman data in °C from Bellanger et al. (2015) and Célini et l. (2023). B) General stratigraphic section of the Vocontian basin and main tectonic events.

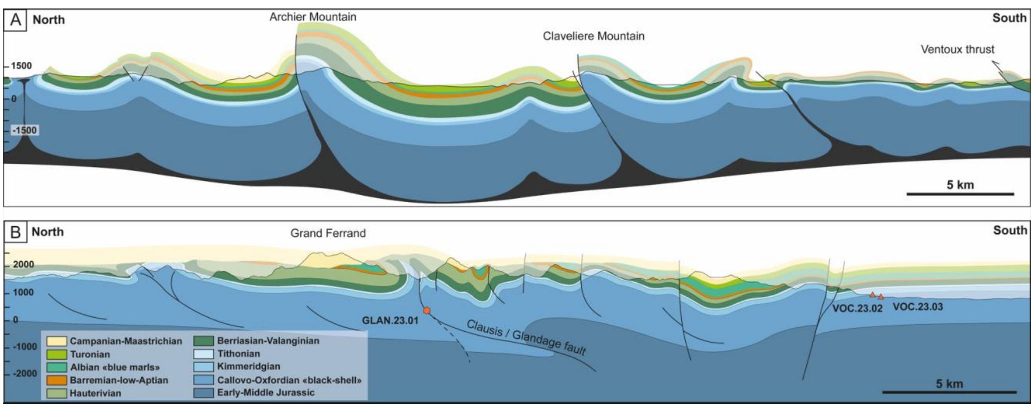

Figure 3: North-South geological cross-section of the Vocontian basin (A) and the Dévoluy massif (B). Location is presented in Fig. 2. Coniacian and Santonian are missing as there is a sedimentary gap (see in the text).

https://doi.org/10.5194/egusphere-2025-3332
Preprint. Discussion started: 28 July 2025

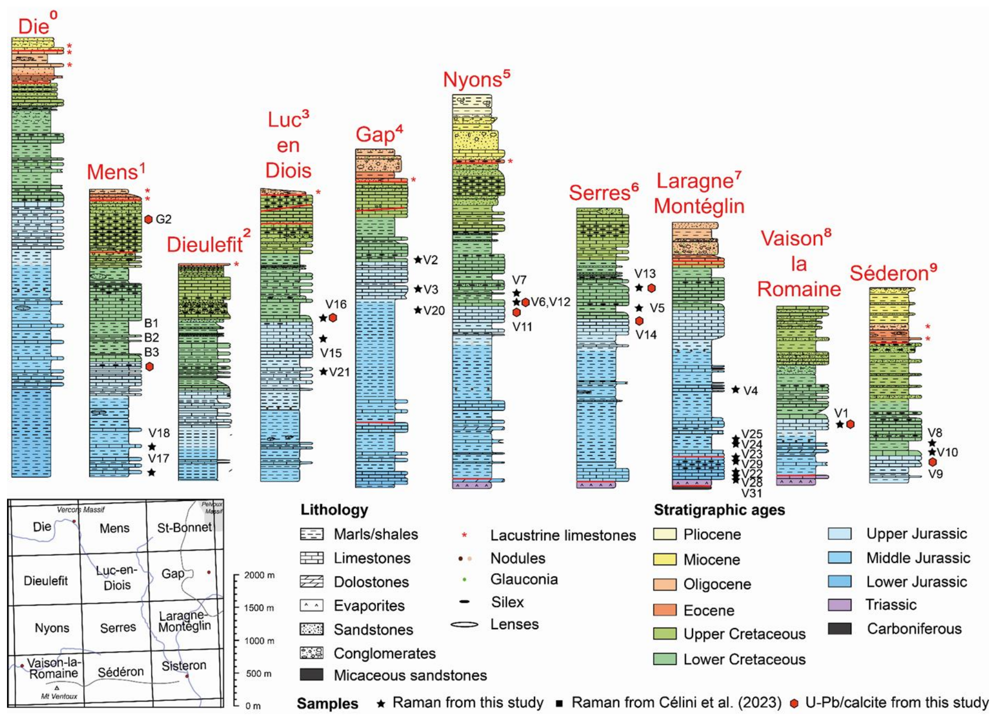

Figure 4: Stratigraphic logs corresponding to each geological notice of BRGM maps from the Vocontian basin. Sample names are shortened from V.23.X to VX for simplification and space in the figure.

https://doi.org/10.5194/egusphere-2025-3332
Preprint. Discussion started: 28 July 2025

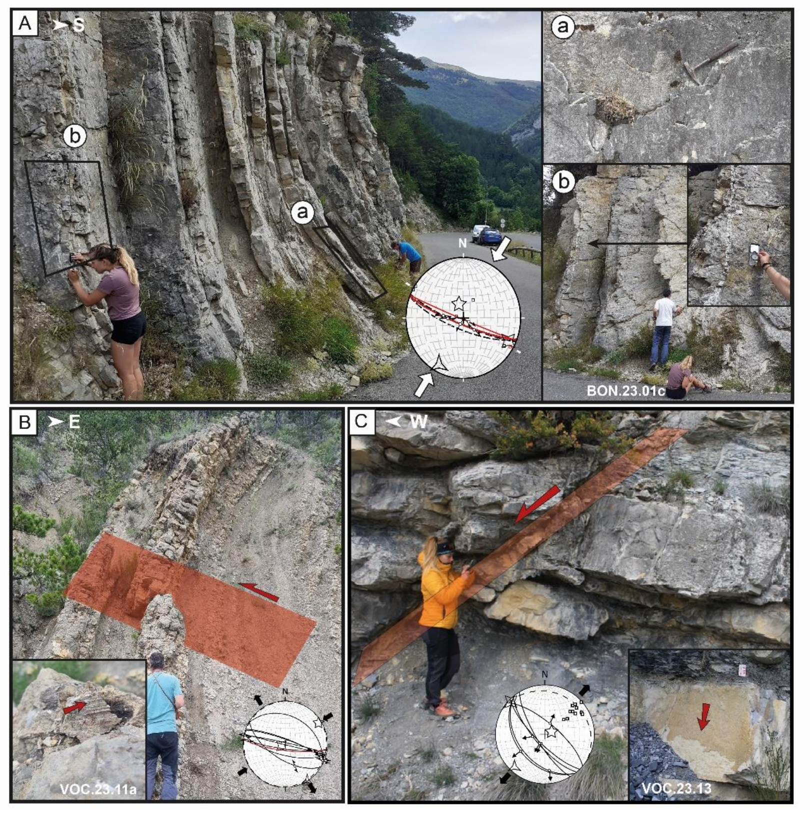

Figure 5: Main geological structures associated to their corresponding measurement and U-Pb age. A) sample BON.23.01. B) sample VOC.23.11. C) sample VOC.23.13.

https://doi.org/10.5194/egusphere-2025-3332
Preprint. Discussion started: 28 July 2025

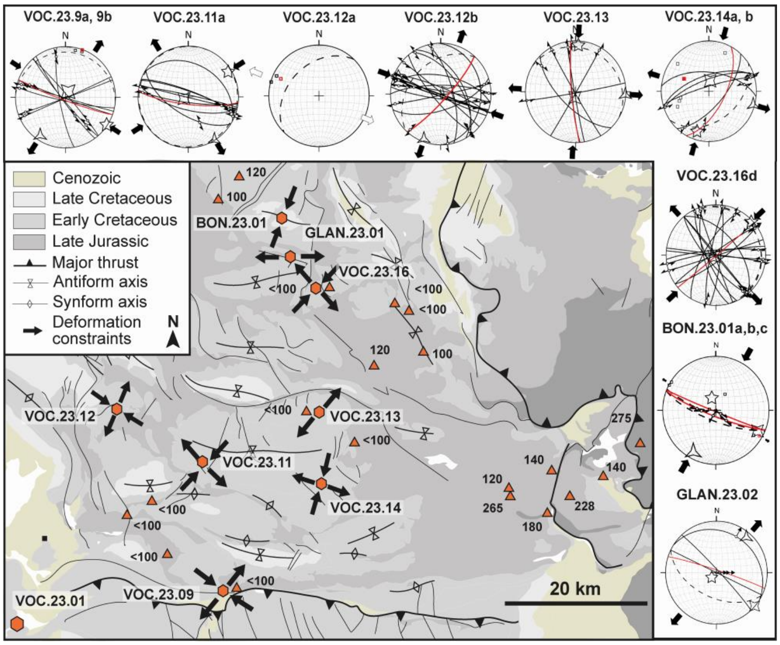

Figure 6: Simplified geological map with structural analysis of each dated sample and location of Raman thermometry results given in °C.

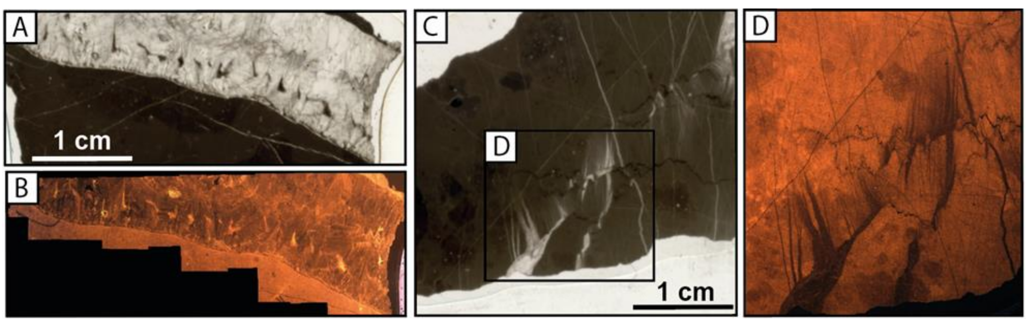

Figure 7: Examples of LPNA (A and C) and cathodolumiscence microphotographs (B and D) of two different types of U/Pb-dated calcite veins. A) and B) sample VOC-23-01. C) and D) sample VOC-23-11a.

https://doi.org/10.5194/egusphere-2025-3332
Preprint. Discussion started: 28 July 2025

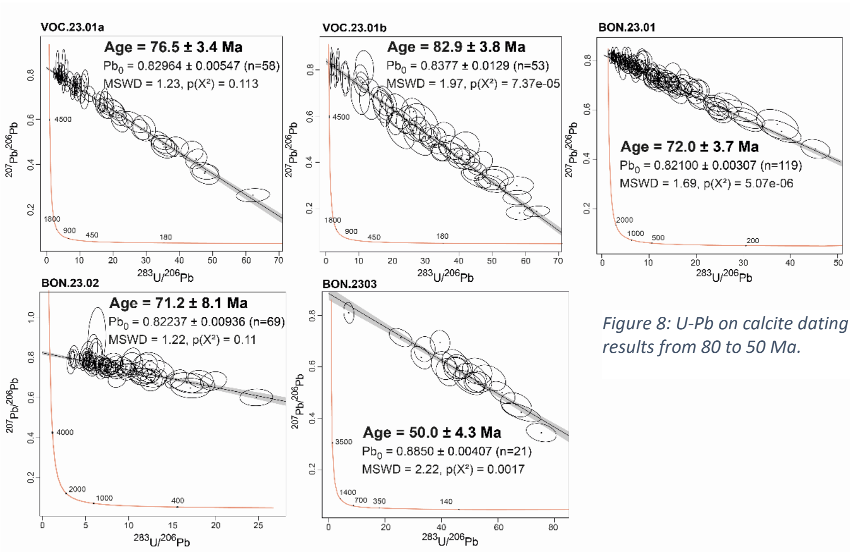

Figure 8: U-Pb on calcite dating results from 80 to 50 Ma.

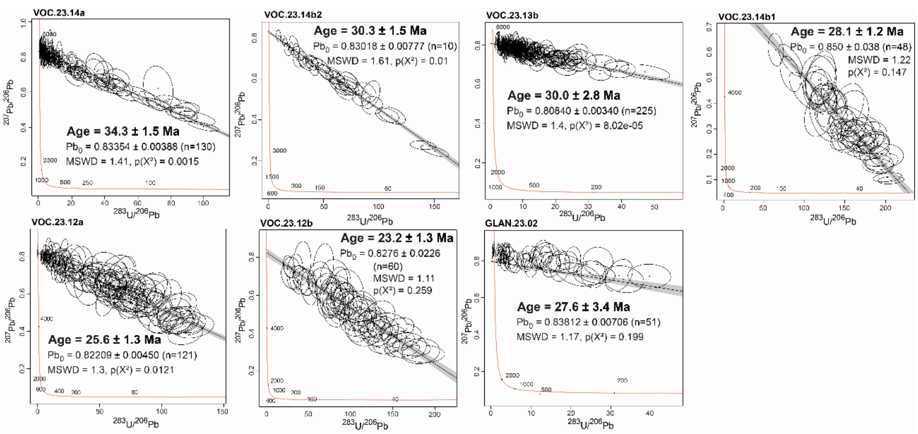

Figure 9: U-Pb on calcite dating results from 30 to 20 Ma.

https://doi.org/10.5194/egusphere-2025-3332
Preprint. Discussion started: 28 July 2025

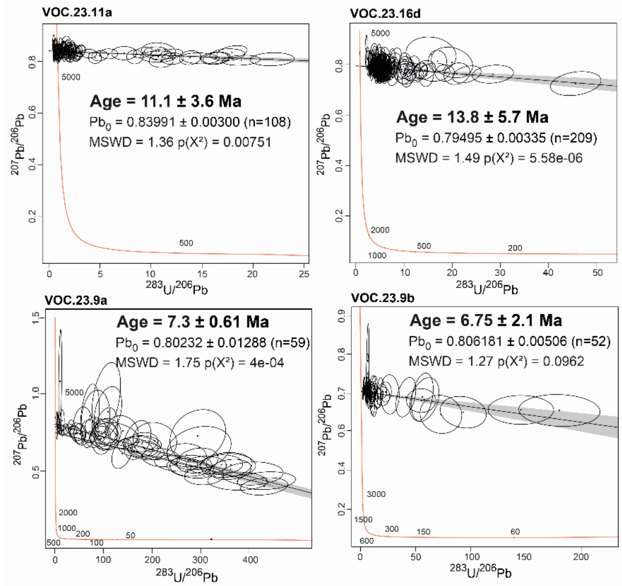

Figure 10: U-Pb on calcite dating results from 12 to 7 Ma.

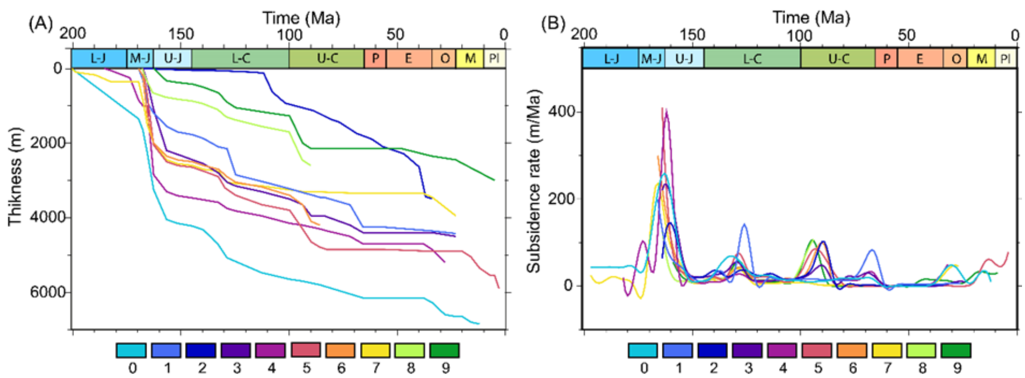

Figure 11: A) Burial history computed after the synthetic stratigraphic sections shown in Figure 10. B) evolution of sediment accumulation rate through time. 0: Die; 1: Dieulefit; 2: Gap; 3: Laragne-Montéglin; 4: Luc-en-Diois; 5: Mens; 6: Nyons; 7: Sédéron; 8: Serre; 9: Vaison-la-Romaine. L: lower, mi: middle; u: upper; J: jurassic; C: cretaceous; p: Paleocene; e: Eocene; o: Oligocene; m: Miocene; pl: Pliocene.

https://doi.org/10.5194/egusphere-2025-3332
Preprint. Discussion started: 28 July 2025

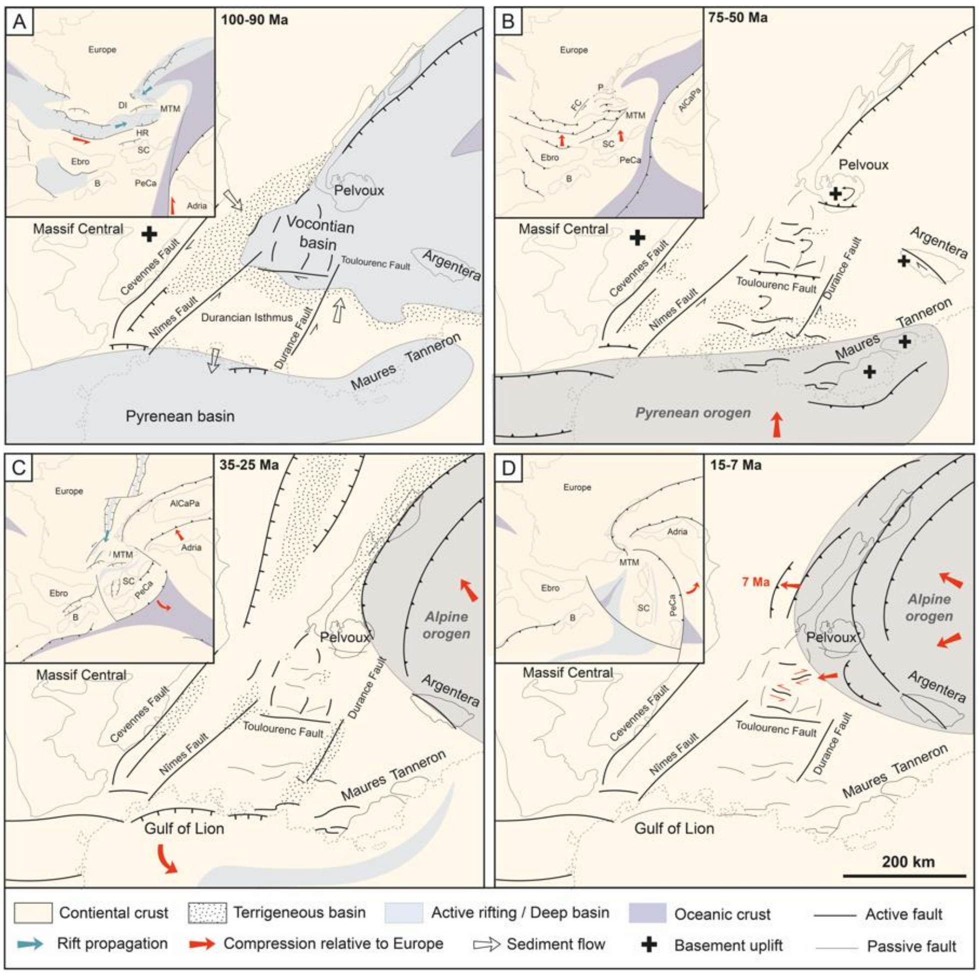

Figure 12: Regional tectonic and paleogeographical reconstitutions of SE France showing the evolution of the Vocontian basin since the Middle Cretaceous (modified after Boschetti et al., 2025b). A) Rifting in overlapping Pyrenean-Vocontian rift segments at 110-90 Ma. B) Pyrenees-Provence collision phase from 75 to 50 Ma. C) Opening of the West European Rift and onset of Alpine foreland fold and thrust belt tectonics. D) Alpine collision and westward propagation of deformation front. SC: Corsica-Sardinia; B: Baleares; C: Chartreuse; V: Vercors.

https://doi.org/10.5194/egusphere-2025-3332
Preprint. Discussion started: 28 July 2025

Table 1: Calcite sample types and correspondinng measurements and ages.

Sample	Lat	Long	Structures	n	σ1	σ2	σ3	ϕ	U-Pb (Ma)	Error (Ma)
VOC.23.01a	44.159326	5.049163	Vein + Strike slip	-	-	-	-	-	76.5	3.4
VOC.23.02b	44.159326	5.049163	Vein	-	-	-	-	-	82.9	3.8
VOC.23.9a	44.190622	5.47628	Strike-slip (Reverse)	13	02/124	80/025	10/214	0.6	7.3	0.61
VOC.23.9b	44.190622	5.47628	Vein (Associated 9a)	11	73/098	16/291	04/200	0.5	6.75	2.1
VOC.23.11a	44.367914	5.352686	Strike-slip (Post-fold)	6	17/0.23	71/185	05/292	0.5	11.1	3.6
VOC.23.12a	44.437467	5.293520	Vein	-	-	-	-	-	25.6	1.3
VOC.23.12b	44.437467	5.293520	Vein + Strike slip	17	10/292	78/078	06/201	0.5	23.2	1.3
VOC.23.13b	44.417889	5.657694	Normal fault	14	78/069	05/315	10/223	0.5	30	2.8
VOC.23.14a	44.328944	5.631972	Vein (Associated 14b)	-	-	-	-	-	34.3	1.5
VOC.23.14b1	44.328944	5.631972	Strike-slip (Normal)	6	17/197	73/007	03/106	0.5	30.3	1.5
VOC.23.14b2	44.328944	5.631972	Strike-slip (Normal)	6	17/197	73/007	03/106	0.5	28.1	1.2
VOC.23.16d	44.575833	5.640667	Strike-slip (Reverse)	20	04/048	86/234	00/138	0.5	13.8	5.7
BON.23.01a	44.62582	5.60985	Plane from fold	11	36/205	04/112	54/017	0.27	72	3.7
BON.23.01	44.62582	5.60985	Plane from fold	11	36/205	04/112	54/017	0.27	71.2	8.1
BON.23.01	44.62582	5.60985	Vein	11	36/205	04/112	54/017	0.27	50	4.3
GLAN.23.02	44.68617	5.59384	Normal fault	4	62/203	04/300	27/032	0.5	27.6	3.4

Table 2: Raman Thermometry data.

Sample	Lat °N	Lon °E	Stratigraphic Age (Ma)	Log/Map	Burial T (30°C/km)	Burial T (60°C/km)	RSCM T (°C)	1s
VOC.23.02	44.556889	5.772778	142	Gap	52	104	<100	
VOC.23.03	44.546834	5.801242	156	Gap	57	114	<100	
VOC.23.05	44.354736	5.668139	135	Serres	51	102	<100	
VOC.23.06	44.296138	5.281886	142	Nyons	51	102	<100	
VOC.23.07	44.299667	5.312604	142	Nyons	51	102	<100	
VOC.23.08	44.227526	5.433728	137	Sederon	75	150	<100	
VOC.23.10	44.221778	5.429244	142	Sederon	77.5	155	<100	
VOC.23.13	44.417889	5.657694	124	Serres	34.5	69	<100	
VOC.23.16	44.575833	5.640667	142	Luc-en-Diois	61.5	123	<100	
VOC.24.17	44.681803	5.414283	167	Mens	122	245	100	20
VOC.24.18	44.698656	5.419786	166	Mens	105	211	120	20
VOC.24.20	44.502694	5.820133	156	Gap	57	114	100	20
VOC.24.21	44.464336	5.697017	157	Luc-en-Diois	69	138	120	20
VOC.24.22	44.316244	5.959372	169	Laragne-Monteglin	93	186	120	20
VOC.24.23	44.308639	5.956206	166	Laragne-Monteglin	73	147	265	12
VOC.24.24a	44.281517	6.014347	163	Laragne-Monteglin	58.5	117	180	20
VOC.24.25	44.294617	6.056911	162	Laragne-Monteglin	58.5	117	228	22
VOCY.24.28a	44.328152	6.128097	170	Laragne-Monteglin	108	216	140	20
VOC.24.29	44.335796	6.020728	166	Laragne-Monteglin	73	147	140	20
VOC.24.31	44.357159	6.166843	175	Laragne-Monteglin	>108	>216	275	6